Audio Engineering Society

Convention Paper

Presented at the 123rd Convention
2007 October 5–8 New York, NY

Extension of an Analytic Secondary Source Selection Criterion for Wave Field Synthesis

Sascha Spors[1]

[1] *Deutsche Telekom Laboratories, Berlin University of Technology, Ernst-Reuter-Platz 7, 10587 Berlin, Germany*

Correspondence should be addressed to Sascha Spors (Sascha.Spors@telekom.de)

ABSTRACT

Wave field synthesis (WFS) is a spatial sound reproduction technique that facilitates a high number of loudspeakers (secondary sources) to create a virtual auditory scene for a large listening area. It requires a sensible selection of the loudspeakers that are active for the reproduction of a particular virtual source. For virtual point sources and plane waves suitable intuitively derived selection criteria are used in practical implementations. However, for more complex virtual source models and loudspeaker array contours the selection is not straightforward. In a previous publication the author proposed a secondary source selection criterion on basis of the sound intensity vector. This contribution will extend this criterion to data-based rendering and focused sources, and will discuss truncation effects.

1. INTRODUCTION

Wave field synthesis is a spatial sound reproduction technique that facilitates a high number of loudspeakers to create a virtual auditory scene for a large listening area. It overcomes some of the limitations of stereophonic reproduction, like e.g. the sweet-spot. The physical foundation of WFS is given by the Kirchhoff- Helmholtz integral. This fundamental principle states that a continuous distribution of dipole and monopole sources (secondary sources) placed around the listening area is required for physically perfect recreation of any desired virtual acoustic scene within the entire listening area. However, for a practical implementation of this principle several simplifications are applied in WFS.

One of these simplifications is to discard one of the two different types of secondary sources. Typically the dipole sources are removed, since monopole sources can be realized reasonable well by loudspeakers with closed cabinets. The Kirchhoff-Helmholtz integral takes inherently care that only those secondary sources are used whose local propagation di-

rection coincides with the wave field to be reproduced. This inherent feature gets lost when using monopoles only. Hence, removing the dipole secondary sources requires to sensibly select the secondary sources used for the reproduction of a particular virtual sound field. Only those sources whose propagation direction coincides with the local propagation direction of the virtual source wave field at the source position should contribute to the reproduction. Typical virtual source models which are used for model-based rendering of acoustic scenes are point sources and plane waves. For these, intuitively derived selection criteria are used in practical implementations. However, for more complex virtual source models, like e. g. [1, 2], the selection might not be straightforward. An sensible selection of active secondary sources is especially required for WFS systems which have bend or closed-form contours, e. g. consist of more than one linear loudspeaker array. In a previous publication [3] the author proposed to use the time-averaged sound intensity vector of the virtual source wave field as analytic secondary source selection criterion. It was shown that the criterion validates the intuitively used criteria for virtual plane waves and point sources placed outside the listening area. This contribution will further investigate and extend this criterion in various aspects.

WFS is capable of reproducing virtual sources which are located within the listening area. These sources are typically referred to as focused sources. This contribution will extend the proposed secondary source selection scheme towards focused virtual sources.

Another issue that is connected to the secondary source selection are truncation artifacts. It will be shown that these artifacts are quite severe for focused sources. A well known countermeasure, weighting of the loudspeaker signals, is investigated as solution to reduce these truncation artifacts.

This paper is organized as follows: Section 2 will introduce the theoretical background of WFS, Section 3 reviews the selection criterion for non-focused sources and extends the previous published work in some aspects. The criterion for non-focused sources is derived in Section 4. The effects of truncation for bend or closed-form WFS systems and countermeasures to these are discussed in Section 5.

2. WAVE FIELD SYNTHESIS

The physical basis of WFS is given by the Kirchhoff-Helmholtz integral [4]

$$P(\mathbf{x},\omega) = -\oint_{\partial V} \left(G_0(\mathbf{x}|\mathbf{x}_0,\omega)\, \frac{\partial}{\partial \mathbf{n}} S(\mathbf{x}_0,\omega) - S(\mathbf{x}_0,\omega)\, \frac{\partial}{\partial \mathbf{n}} G_0(\mathbf{x}|\mathbf{x}_0,\omega) \right) dS_0 \,, \quad (1)$$

where $P(\mathbf{x},\omega)$ denotes the pressure field inside a bounded region V surrounded by the border ∂V, $G_0(\mathbf{x}|\mathbf{x}_0,\omega)$ the free-field Green's function, $S(\mathbf{x},\omega)$ the wave field of the virtual source and $\frac{\partial}{\partial \mathbf{n}}$ the directional gradient in direction of the normal vector $\mathbf{n}$. Figure 1 illustrates the geometry. The wave field outside of V is zero and V is assumed to be source-free.

The Green's function $G_0(\mathbf{x}|\mathbf{x}_0,\omega)$ characterizes the wave field emitted by a monopole source placed at the position $\mathbf{x}_0$, its directional gradient the field of a dipole source. The Kirchhoff-Helmholtz integral can be interpreted as follows: A distribution of suitable driven monopole and dipole sources placed around a desired listening area V is sufficient for recreation of a desired virtual source within the entire listening area. For WFS several simplifications of this basic principle are typically applied [5, 6, 7]:

1. elimination of dipole secondary sources,
2. sampling of secondary source contour, and
3. usage of secondary point sources for two-dimensional reproduction.

The first simplification will be discussed in detail in the remainder of this paper. The second accounts for the fact that secondary sources (loudspeakers) can only be placed at discrete positions. This implies a spatial sampling of the continuous secondary source distribution in the Kirchhoff-Helmholtz integral. A consequence of this may be spatial aliasing artifacts being present in the reproduced wave field. These artifacts have been discussed e. g. in [8, 9]. The third simplification is related to the choice of secondary sources. For two-dimensional reproduction line source would be the appropriate choice as secondary sources. However, two-dimensional WFS utilizes point sources (closed loudspeakers) instead

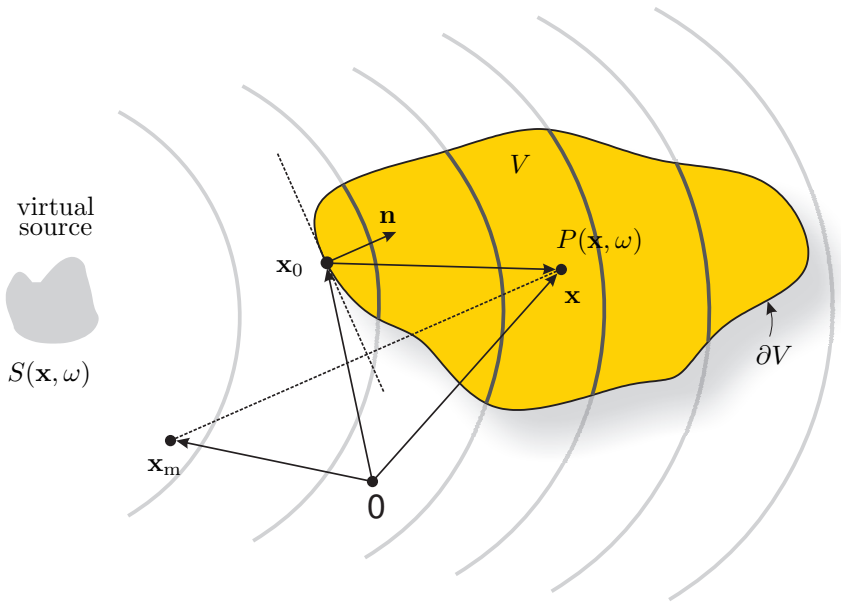

Fig. 1: Geometrical parameters used for the Kirchhoff-Helmholtz integral (1) and monopole only reproduction.

of secondary line sources for reproduction. Please see e. g. [5, 6, 9] for more details. The latter two simplifications will have no influence on the proposed selection scheme. Within the context of this paper the elimination of dipole secondary sources only and the resulting implications for WFS rendering algorithms are discussed.

The second term in the Kirchhoff-Helmholtz integral (1) belonging to the dipole secondary sources can be eliminated by modifying the Green's function used [5, 6, 7]. The modified Green's function $G'(\mathbf{x}|\mathbf{x}_0,\omega)$ has to obey the following condition

$$\frac{\partial}{\partial \mathbf{n}} G'(\mathbf{x}|\mathbf{x}_0,\omega)\Big|_{\mathbf{x}_0\in\partial V} = 0\,, \qquad (2)$$

in order to eliminate the dipole secondary sources. Condition (2) formulates a homogeneous Neumann boundary condition imposed on ∂V, hence the boundary ∂V will be implicitly modeled as acoustically rigid surface. The desired Green's function is derived by adding a suitable homogeneous solution (with respect to the region V) to the free-field Green's function

$$G'(\mathbf{x}|\mathbf{x}_0,\omega) = G_0(\mathbf{x}|\mathbf{x}_0,\omega) + G_0(\mathbf{x}_\mathrm{m}(\mathbf{x})|\mathbf{x}_0,\omega)\,. \qquad (3)$$

A solution fulfilling Eq. (2) is given by choosing the receiver point $\mathbf{x}_\mathrm{m}(\mathbf{x})$ as the point $\mathbf{x}$ mirrored at the tangent to the curve ∂V at the position $\mathbf{x}_0$ (see Fig. 1). Note, that due to the specialized geometry $G'(\mathbf{x}|\mathbf{x}_0,\omega) = 2\,G_0(\mathbf{x}|\mathbf{x}_0,\omega)$. The elimination of the secondary dipole sources has two consequences: (1) the wave field outside of V is a mirrored version of the wave field inside V and (2) without modification undesired reflections will be reproduced. The first consequence implies that the boundary ∂V has to be convex, the second implies a modification of the driving function as will be shown in the following.

As mentioned before, the surface ∂V will be implicitly modeled as rigid surface when discarding the secondary dipoles. Hence, the reproduction of the desired wave field will be superimposed by undesired reflections produced by the (virtual) boundary ∂V. These reflections will only take place for those secondary sources where the local propagation direction of the virtual wave field does not coincide with the normal vector $\mathbf{n}$ of the secondary source. Since we are free to choose the secondary sources used for reproduction, these undesired reflections can be avoided by discarding those secondary sources which reproduce the reflections. This selection can be for-

mulated by introducing a window function $a(\mathbf{x}_0)$ into the secondary source driving function $D(\mathbf{x}_0, \omega)$

$$P(\mathbf{x}, \omega) = - \oint_{\partial V} \underbrace{2a(\mathbf{x_0}) \frac{\partial}{\partial \mathbf{n}} S(\mathbf{x}_0, \omega)}_{D(\mathbf{x}_0, \omega)} G(\mathbf{x}|\mathbf{x}_0, \omega)\, dS_0 \,, \quad (4)$$

where

$$a(\mathbf{x}_0) = \begin{cases} 1 & \text{, if the local propagation direction} \\ & \text{of } S(\mathbf{x_0}, \omega) \text{ coincides with } \mathbf{n}, \\ 0 & \text{, otherwise.} \end{cases} \quad (5)$$

This definition of the window function is obvious but not useful for practical reproduction algorithms since it is not formulated analytically. The following sections will introduce analytical definitions of the window function $a(\mathbf{x}_0)$.

3. SECONDARY SOURCE SELECTION FOR NON-FOCUSED SOURCES

The following section introduces an analytic secondary source selection scheme for non-focused sources and will illustrate its application to model- and data-based rendering of virtual scenes.

3.1. Secondary Source Selection Criterion

The basic idea to derive an analytic secondary source selection criterion is to utilize the acoustic intensity vector $\mathbf{i}(\mathbf{x}, t) = p(\mathbf{x}, t)\, \mathbf{v}(\mathbf{x}, t)$ for selection of the active secondary sources. The acoustic intensity vector $\mathbf{i}(\mathbf{x}, t)$ represents the instantaneous amount of energy flow per unit time and area with respect to direction. The intensity vector points into the direction of increased energy density. Hence, $\mathbf{i}(\mathbf{x}, t)$ can be used to characterize the traveling direction of acoustic waves. However, it is useful to average the intensity vector $\mathbf{i}(\mathbf{x}, t)$ over a signal period. The time averaged acoustic intensity vector is defined as follows [4]

$$\bar{\mathbf{i}}(\mathbf{x}, t) = \frac{1}{T} \int_0^T p(\mathbf{x}, t)\, \mathbf{v}(\mathbf{x}, t)\, dt \,, \quad (6)$$

where T denotes the signal period. The time averaging process is conveniently formulated in the frequency domain by transforming the pressure and velocity vector using the Fourier transformation. The time averaged acoustic intensity vector $\bar{\mathbf{I}}_\mathrm{S}(\mathbf{x}, \omega)$ for the virtual source is then given as

$$\bar{\mathbf{I}}_\mathrm{S}(\mathbf{x}, \omega) = \frac{1}{2} \Re\{ S(\mathbf{x}, \omega) \mathbf{V}_\mathrm{S}(\mathbf{x}, \omega)^* \} \,, \quad (7)$$

where $\Re\{\cdot\}$ denotes the real part of its argument and the superscript $*$ the conjugate complex function. The window function is defined straightforward on the basis of condition (5) using the time-averaged acoustic intensity as

$$a(\mathbf{x}_0) = \begin{cases} 1 & \text{, if } \langle \bar{\mathbf{I}}(\mathbf{x}_0, \omega), \mathbf{n}(\mathbf{x}_0) \rangle > 0, \\ 0 & \text{, otherwise.} \end{cases} \quad (8)$$

where $\langle \cdot, \cdot \rangle$ denotes the inner product of two vectors. In the next section this definition will be applied to two analytic virtual source models (plane wave, point source) frequently used in model-based rendering. Additionally, its application to data-based rendering will be illustrated.

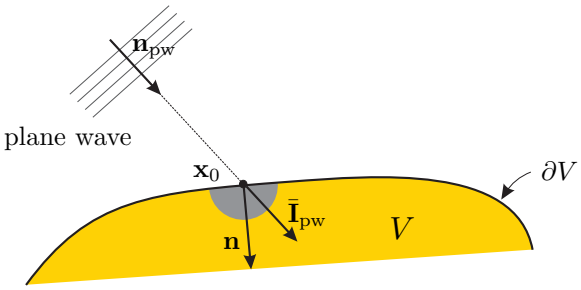

Fig. 2: Secondary source selection criterion for virtual plane waves. The gray wedge illustrates the selection criterion.

3.2. Secondary Source Selection for Virtual Plane Waves

The wave field of a monochromatic plane wave is given as follows [4]

$$S_\mathrm{pw}(\mathbf{x}, \omega) = \hat{S}(\omega)\, e^{-j \mathbf{k}_\mathrm{pw}^T \mathbf{x}} \,, \quad (9)$$

where $\hat{S}(\omega)$ denotes the spectrum of the plane wave, $\mathbf{k}_\mathrm{pw} = \frac{\omega}{c} \mathbf{n}_\mathrm{pw}$ the wave vector of the plane wave and $\mathbf{n}_\mathrm{pw}$ its normal vector (propagation direction). Figure 2 illustrates the geometry. The time averaged acoustic intensity for a plane wave is given by introducing (9) and its velocity vector into (7) as

$$\bar{\mathbf{I}}_\mathrm{pw}(\mathbf{x}, \omega) = \left| \hat{S}(\omega) \right|^2 \frac{1}{2\rho_0 c}\, \mathbf{n}_\mathrm{pw} \,. \quad (10)$$

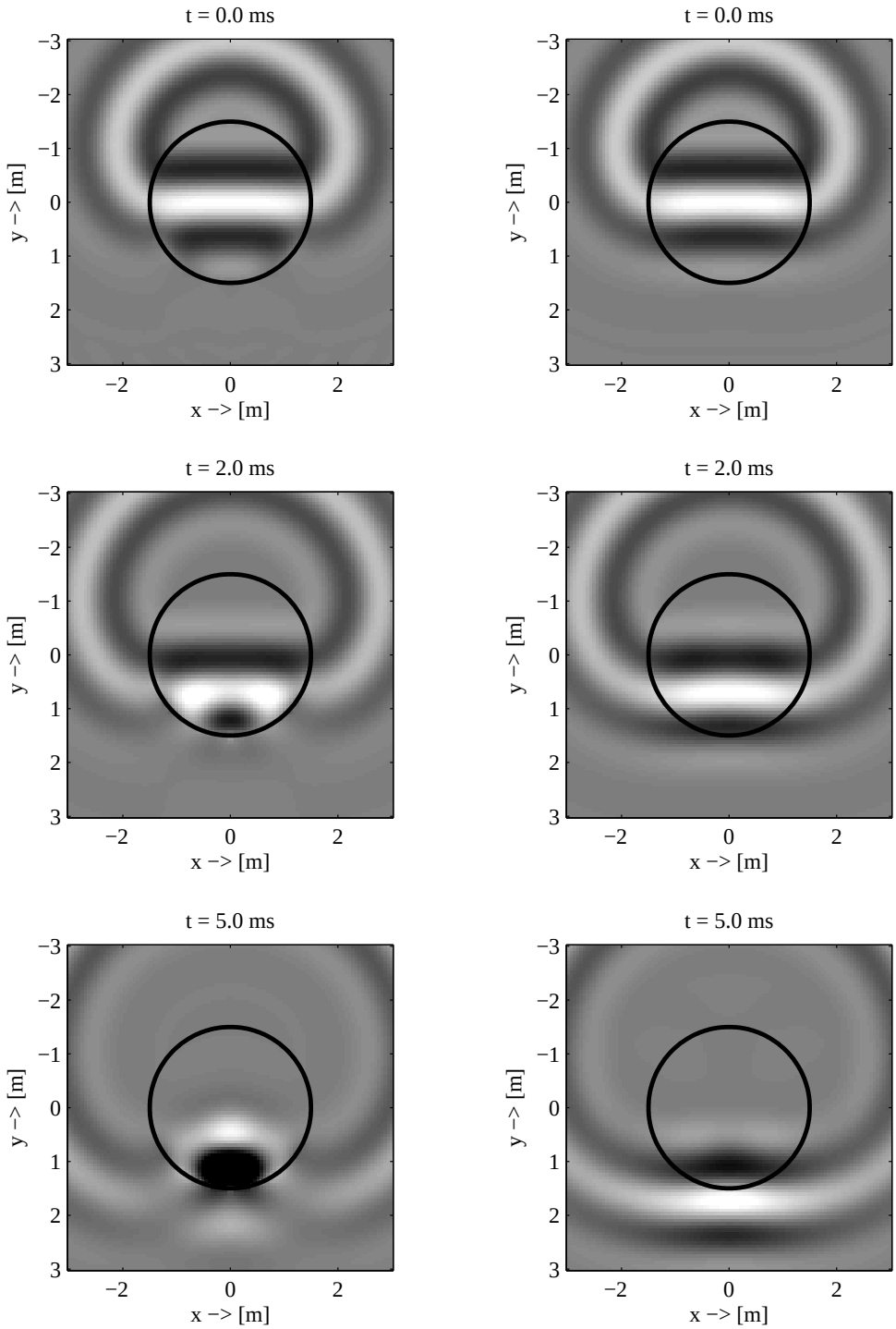

Fig. 3: Reproduction of a band-limited (sinc shaped) plane wave using a circular distribution of secondary monopole sources ($R = 1.50$ m). The left row shows the reproduced wave field when driving all secondary sources, the right row when applying the proposed secondary source selection scheme.

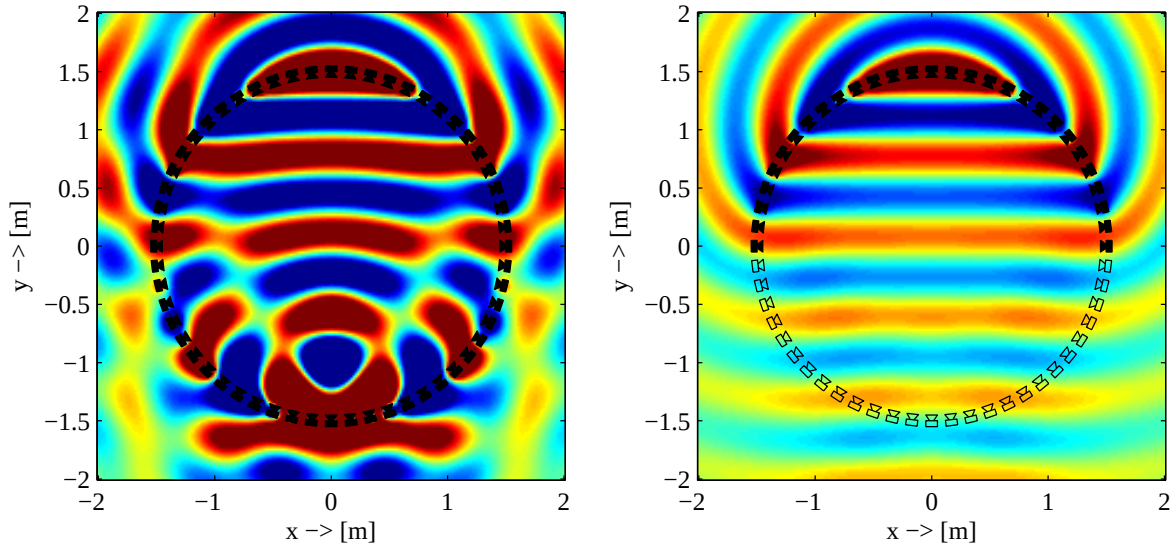

(a) without selection (b) with selection

Fig. 4: Wave field reproduced for a monochromatic virtual plane wave ($f = 500$ Hz) without and with appropriate selection of active secondary sources. The active secondary sources are indicated by the filled loudspeaker symbols.

Note that $\bar{\mathbf{I}}_{\mathrm{pw}}(\mathbf{x}, \omega)$ is independent from the actual position $\mathbf{x}$. Accordingly to Eq. (8), a secondary source is selected if the normal vector $\mathbf{n}$ of the secondary source and the propagation direction of the plane wave $\mathbf{n}_{\mathrm{pw}}$ form an acute-angle. This condition is illustrated by the gray wedge in Fig. 2. To the knowledge of the author, the derived selection scheme is in conjunction with the state of the art used in practical implementations.

Figure 3 and 4 illustrate the effect of the proposed secondary source selection criterion when reproducing a virtual plane wave. Figure 3 shows the reproduction of a band-limited Dirac shaped plane wave using a circular distribution of secondary line sources. The left row illustrates the effect when using all secondary sources, the right row when applying the proposed selection scheme. It can be seen clearly that a reproduction without proper selection of active secondary sources will result in a (virtual) reflection reproduced by the lower part of the loudspeaker array.

Figure 4 illustrates the wave field reproduced by a circular WFS system for a monochromatic virtual plane wave without and with selection of active secondary sources. The simulated WFS system consists of $N = 56$ point sources located on a circle with a radius of $R = 1.50$ m, the frequency of the monochromatic plane wave is $f = 500$ Hz. The geometry of the simulated system is in conjunction with the WFS system at the Deutsche Telekom Laboratories. The reflections reproduced by the lower half-circle of secondary sources can be seen clearly in Fig. 4(a). The wave field within the listening area is deteriorated by the undesired components of the reproduced wave field. Figure 4(b) illustrates the application of the proposed selection scheme. The undesired reflections are removed effectively.

3.3. Secondary Source Selection for Virtual Point Sources

The wave field of a point source is given as follows [4]

$$S_{\mathrm{ps}}(\mathbf{x}, \omega) = \hat{S}(\omega)\, \frac{1}{r}\, e^{-j\frac{\omega}{c}r}\,, \tag{11}$$

where $r = |\mathbf{x} - \mathbf{x}_{\mathrm{ps}}|$ denotes the distance between an observation point $\mathbf{x}$ and the virtual source position $\mathbf{x}_{\mathrm{ps}}$. Only non-focused point sources with source positions outside the listening area ($\mathbf{x}_{\mathrm{ps}} \notin V$) will be discussed in this section. The time averaged acoustic

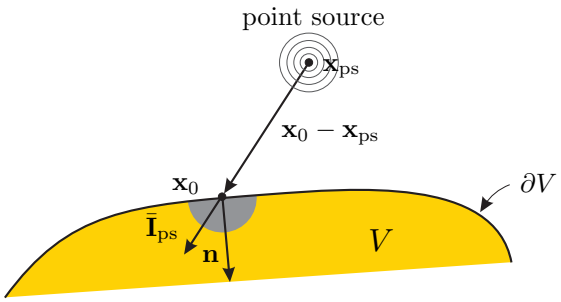

Fig. 5: Secondary source selection criterion for virtual point sources. The gray wedge illustrates the selection criterion.

intensity for a point source is derived by introducing is pressure (11) and velocity vector into Eq. (7) as

$$\bar{\mathbf{I}}_{\mathrm{ps}}(\mathbf{x},\omega) = \left|\hat{S}(\omega)\right|^2 \frac{1}{2\rho_0 c}\,\frac{1}{r^2}\,\underbrace{\frac{\mathbf{x}-\mathbf{x}_{\mathrm{ps}}}{|\mathbf{x}-\mathbf{x}_{\mathrm{ps}}|}}_{\vec{e}_r}\,, \qquad (12)$$

where $\vec{e}_r$ denotes the outward pointing radial vector of the point source. Evaluating the acoustic intensity of a point source (12) at the secondary source position and application of condition (8) yields the secondary source selection criterion for point sources. Hence, a secondary source is selected if the normal vector $\mathbf{n}$ of the secondary source and the outward pointing radial vector $\vec{e}_r$ of the point source form an acute-angle. Figure 5 illustrates the geometry of the derived condition, the gray wedge shows the selection scheme. Figure 6 illustrates the effect of the proposed selection criterion on the reproduced wave field for a monochromatic virtual point source. The geometry of the simulated circular WFS system is equal to Fig. 4 ($N = 56$, $R = 1.50$ m), the position of the monochromatic virtual point source ($f = 500$ Hz) is $\mathbf{x}_{\mathrm{ps}} = [0\ 2]^T$ m. The reflections emerging from the lower part of the array can be seen clearly in Fig. 6(a). The secondary source selection criterion eliminates these reflections effectively, as can be observed in Fig. 6(b). The level of the reflections is lower in Fig. 6(a) than for the case of a virtual plane wave shown in Fig. 4(a). This is due to the fact that the amplitude of the virtual point source decays over distance. As a result the lower secondary sources are driven with a lower source strength in comparison with a virtual plane wave, which exhibits no decay over distance.

3.4. Secondary Source Selection for Data-based Rendering

In data-based rendering the virtual wave field is typically captured by measurement or simulation of an (complex) acoustic scene. The secondary source selection criterion derived for virtual plane waves in Section 3.2 can be applied to data-based rendering as will be shown in the following.

Arbitrary wave fields can be decomposed into a superposition of orthogonal contributions. The different eigensolutions of the wave equation for different coordinate systems are often used for this purpose. For spherical and Cartesian coordinates these eigensolutions are spherical harmonics and plane waves, respectively [4]. The decomposition of the virtual wave field into plane waves is often being used in data-based rendering [10].

For two-dimensional wave fields this decomposition can be formulated as [5]

$$P(\mathbf{x},\omega) = \frac{k}{(2\pi)^2}\int_0^{2\pi} \bar{P}(\theta,\omega) e^{-jkr\cos(\theta-\alpha)}\,d\theta\,, \qquad (13)$$

where $\bar{P}(\theta,\omega)$ denotes the plane wave decomposition coefficients and α, r the polar coordinates of $\mathbf{x} = [x\ y]^T$ with $x = r\cos\alpha$, $y = r\sin\alpha$. The plane wave decomposition coefficients $\bar{P}(\theta,\omega)$ can be interpreted as the spectrum of a plane wave with incidence angle θ. Hence, Eq. (13) can be interpreted as a superposition of plane waves with spectrum $\bar{P}(\theta,\omega)$ from all possible directions. The plane wave decomposition coefficients are given as

$$\bar{P}(\theta,\omega) = \int_0^{\infty}\int_0^{2\pi} P(\mathbf{x},\omega)\, e^{jkr\cos(\theta-\alpha)}\, r\, d\alpha\, dr\,. \qquad (14)$$

The plane wave decomposition coefficients can be measured conveniently by circular microphone arrays as shown e. g. in [10].

The driving function for a plane wave decomposed virtual wave field can be derived from Eq. (13) by (1) calculating its directional gradient, (2) evaluating the resulting function at the secondary source position $\mathbf{x}_0$ and (3) only taking those plane wave components into account which fulfil the selection criterion derived for plane waves in Section 3.2. Performing these steps yields the driving function for a

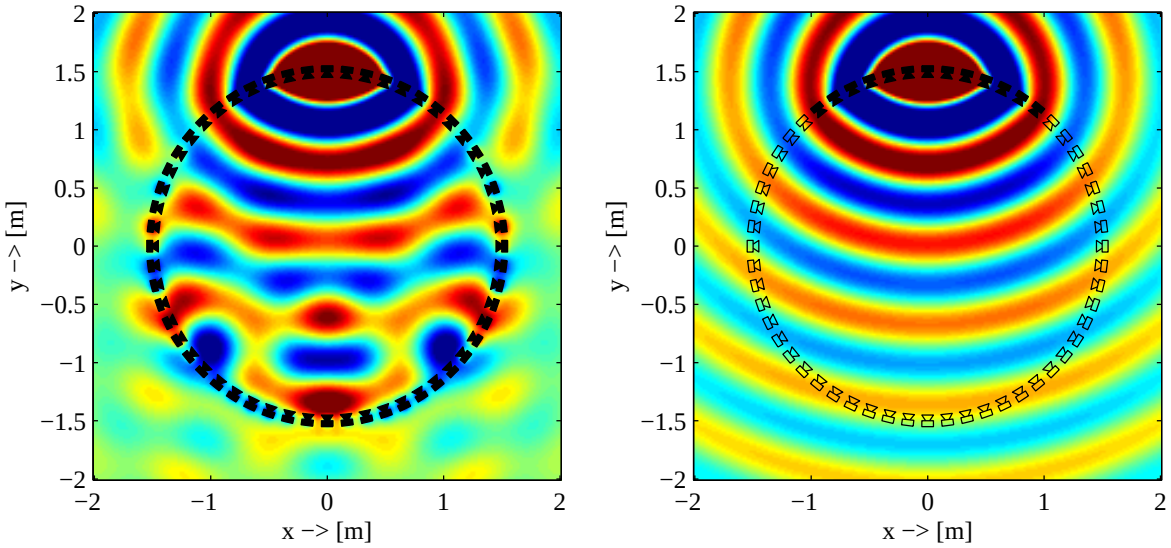

(a) without selection (b) with selection

Fig. 6: Wave field reproduced for a monochromatic virtual point source ($f = 500$ Hz) at $\mathbf{x}_{\text{ps}} = [0\ 2]^T$ m without and with selection of active secondary sources. The active secondary sources are indicated by the filled loudspeaker symbols.

plane wave decomposed virtual wave field $S(\mathbf{x}, \omega)$ as

$$D(\mathbf{x}_0, \omega) = -\frac{jk^2}{(2\pi)^2} \times \\ \times \int_{\gamma-\frac{\pi}{2}}^{\gamma+\frac{\pi}{2}} \bar{S}(\theta, \omega)\ \cos(\theta - \gamma)\, e^{-jkr_0 \cos(\theta-\alpha_0)}\, d\theta\ , \tag{15}$$

where γ denotes the angle of the normal vector $\mathbf{n}$ of the secondary source and $\bar{S}(\theta, \omega)$ the plane wave decomposition coefficients of the virtual wave field. The virtual wave field should have no source contributions inside the listening area V.

4. SECONDARY SOURCE SELECTION FOR FOCUSED SOURCES

The secondary source selection schemes presented so far assume that the virtual sources are located outside the listening area V. The following will extend the proposed criterion to sources which are located within the listening area.

4.1. Focused Sources

WFS allows, under certain limitations, to auralize virtual sources which are located within the listening area. Typically the point source model is used as desired spatial characteristic for these sources, and the auralized virtual source is commonly termed as focused point source. The derivation of the driving function for a focused point source reproduced by linear secondary source contour is given e. g. in [9]. It is based on the principle of time-delay law focusing or more generally on the principle of time-reversal acoustic focusing [11, 12]. Both methods are frequently applied in e. g. seismic exploration or medical imaging.

The driving function of a focused point source at the position $\mathbf{x}_{\text{fs}} \in V$ is derived by evaluating the driving function of a virtual point source at $\mathbf{x}_{\text{fs}}$, by reversing the time and introducing a delay. The delay has to ensure causality and should cover at least the minimum travel time of sound from the position of the focused source to the nearest active secondary source. The secondary sources are driven such that they create a wave field that converges towards the focus point $\mathbf{x}_{\text{fs}}$. After the focus point the field diverges again like a point source located at the focus point. The wavefronts are traveling from the secondary sources to the focus point. As a conse-

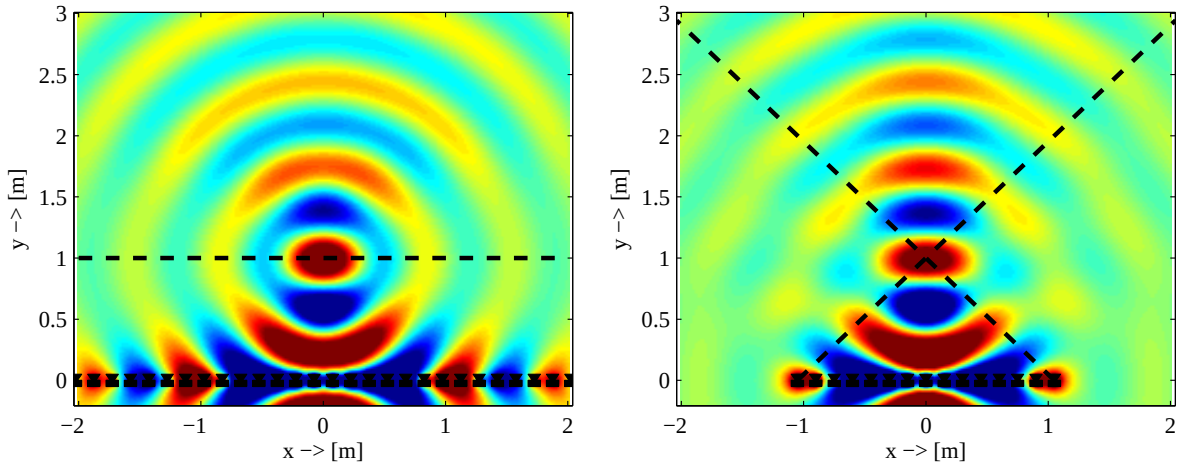

(a) without truncation

(b) truncated at total length $L = 2.10$ m

Fig. 7: Wave field reproduced for a monochromatic focused source ($f = 500$ Hz) placed at $\mathbf{x}_{\text{fs}} = [0\ 1]^T$ m without and with truncation of a linear secondary source distribution. The listening area is indicated by the dashed lines.

quence, the auralization of a focused point source is only correct if the focused source is located between the secondary sources and the listener [9]. Figure 7(a) illustrates the wave field reproduced by a linear secondary source distribution of infinite length. The secondary sources (point sources) are located on the x-axis of the coordinate system, the distance between them is $\Delta x = 15$ cm. A monochromatic focused source is reproduced at the position $\mathbf{x}_{\text{fs}} = [0\ 1]^T$ m.

It can be concluded from Fig. 7(a) and from the properties of focused sources discussed above that these sources only exhibit the characteristics of a point source in the half-space which is delimited by a line (plane) through the position of the focused source which is parallel to the loudspeaker array (see dashed line in Fig. 7(a)). Hence, the reproduced focused source does not exhibit the omnidirectional characteristic of a real point source.

Practical realizations of linear secondary source contours will be of finite length. This truncation limits the listening area further. Figure 7(b) illustrates the wave field reproduced by a truncated linear loudspeaker array with a total length of $L = 2.10$ m. The effective listening area can be approximated geometrically, as indicated in the figure by the dashed lines. It is given as the space in between the upper triangle. As for non-focused sources, no selection of active secondary sources is required for a WFS system consisting only of one linear secondary source distribution. All secondary sources are used in this situation.

Using the time-reversal principle, the derivation of the driving function for a linear secondary source contour and focused sources can be generalized straightforward to arbitrary shaped secondary source contours ∂V. However, no inherent secondary source selection scheme emerges from the time-reversal principle. In order to maintain the auralization of a focused source for a specific listener position, care has to be taken to create wavefronts with a corresponding traveling direction. Due to the effects outlined above for focused sources reproduced on linear secondary source contours, a sensible selection of active secondary sources is necessary for focused point sources and bend secondary source contours. A selection criterion will be proposed in the following section.

Note, that acoustic focusing in seismic or medical applications is often used without selection of active secondary sources. Typically the goal is here to create an acoustic singularity for analysis of layered media or for destroying kidney stones. A controlled propagation direction of the focused source towards

an observer does not play a major role in these applications.

4.2. Secondary Source Selection Criterion for Focused Sources

In the following, a secondary source criterion for focused sources and arbitrary shaped secondary source contours will be proposed. As discussed in the previous section, focused sources are only auralized correctly if they are located in between the listener and the secondary sources. Only in this situation, the wavefronts travel from the position of the focused source towards the listener. Therefore for the reproduction of focused sources a listener position has to be assumed. The maximum obtainable listening area for a focused source is given by the half-space which is delimited by a line (plane) through the focused source position. In principle, the orientation of this line can be chosen freely for a closed secondary source contour. In the following, the orientation of this line will be denoted by its normal vector $\mathbf{n}_{\text{fs}}$. Figure 8 illustrates the geometry for an arbitrary shaped secondary source contour ∂V. The normal vector $\mathbf{n}_{\text{fs}} = [\cos(\alpha_{\text{fs}}) \;\; \sin(\alpha_{\text{fs}})]^T$ denotes the main propagation direction α_{fs} of the focused source.

The selection of active secondary sources for a particular focused source is performed on basis of (1) the virtual source position $\mathbf{x}_{\text{fs}}$ and (2) its normal vector $\mathbf{n}_{\text{fs}}$. Only those secondary sources should contribute to the focused source whose local propagation direction in the focus point $\mathbf{x}_{\text{fs}}$ coincides with the normal vector $\mathbf{n}_{\text{fs}}$. As shown for non-focused sources, the time-averaged acoustic intensity vector can be used to characterize the local propagation direction. The time-averaged acoustic intensity vector for a point source is given by Eq. (12). Assuming that point sources are used as secondary sources, the acoustic intensity of a secondary source is given as

$$\bar{\mathbf{I}}_0(\mathbf{x},\omega) = |D_{\text{fs}}(\mathbf{x}_0,\omega)|^2 \, \frac{1}{2\rho_0 c} \, \frac{1}{r^2} \, \frac{\mathbf{x}-\mathbf{x}_0}{|\mathbf{x}-\mathbf{x}_0|} \,, \quad (16)$$

where $D_{\text{fs}}(\mathbf{x}_0,\omega)$ denotes the driving function of a focused source. Hence, the secondary source selection criterion for a focused source can be derived as

$$a(\mathbf{x}_0) = \begin{cases} 1 & \text{, if } \langle \bar{\mathbf{I}}_0(\mathbf{x}_{\text{fs}},\omega), \mathbf{n}_{\text{fs}} \rangle > 0, \\ 0 & \text{, otherwise.} \end{cases} \quad (17)$$

The gray wedge in Fig. 8 illustrates the secondary source selection criterion.

Figure 9 illustrates the effect of the proposed selection criterion on the reproduced wave field for a monochromatic focused source. The geometry of the simulated circular WFS system is equal to Fig. 4 ($N = 56$, $R = 1.50$ m), the position of the monochromatic focused source ($f = 500$ Hz) is $\mathbf{x}_{\text{fs}} = [0 \;\; 0.5]^T$ m, the normal vector $\mathbf{n}_{\text{fs}} = [\cos(\alpha_{\text{fs}}) \;\; \sin(\alpha_{\text{fs}})]^T$ with $\alpha_{\text{fs}} = -90^{\text{o}}$. The wave field reproduced without applying the selection criterion (17) shown in Fig. 9(a) looks correct on first sight. However, the (primary) wave fronts travel from all directions towards the focus point. Figure 9(b) shows the reproduced wave field when using the proposed selection criterion. The listening area is indicated by the dashed line. Below this line and within the circular secondary source contour all wave fronts exhibit the correct traveling direction. The artifacts that can be seen in the wave field are due to truncation effects. These artifacts and countermeasures will be discussed in Section 5.

Figure 9 illustrates the effect of different normal vectors $\mathbf{n}_{\text{fs}}$ on the selection of active secondary sources and the reproduced wave field.

Most of the current WFS implementations, the author has knowledge of the details, assume for focused sources that the listener is located in a pre-defined position (often the center of the system). The normal vector $\mathbf{n}_{\text{fs}}$ is then given as the normalized vector from the position of the focused source to the assumed listener position. Therefore, the selection scheme proposed in this paper provides some new degrees of freedom for focused sources by providing the possibility to choose its main propagation direction.

Note, that a limited aperture may further limit the effective listening area for a focused source. This was illustrated in the previous section at the example of a linear secondary source contour (see Fig. 7(b)).

5. TRUNCATION ARTIFACTS

Practical implementations of non-closed secondary source contours will always be of finite length. The effects emerging from the truncation of linear secondary source contours used for WFS have been investigated in detail by [13, 9, 14]. The resulting artifacts in the reproduced wave field are referred to as truncation artifacts in the context of WFS.

This section briefly discusses the truncation artifacts of closed secondary source contours and potential

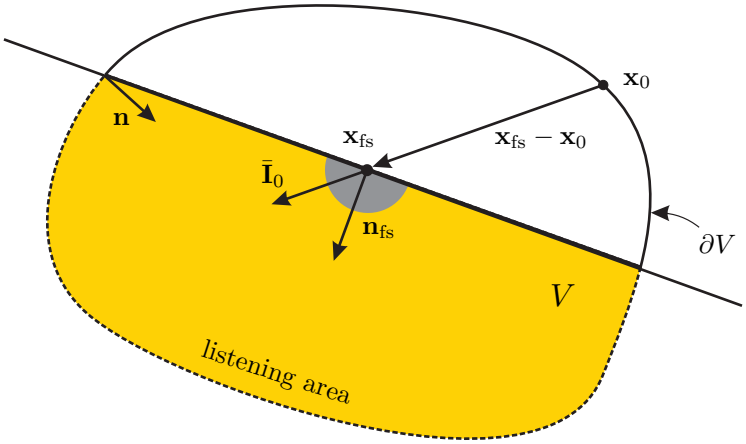

Fig. 8: Secondary source selection criterion for focused sources. The gray wedge illustrates the proposed selection scheme.

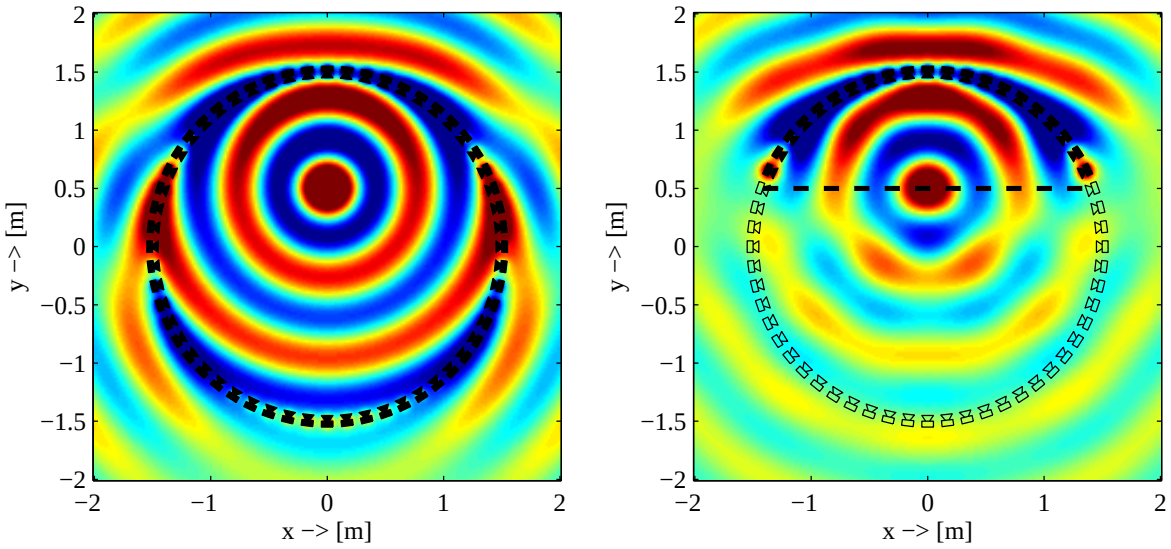

(a) without selection

(b) with selection ($\alpha_{\text{fs}} = -90^{\text{o}}$)

Fig. 9: Wave field reproduced for a monochromatic focused source ($f = 500$ Hz) placed at $\mathbf{x}_{\text{fs}} = [0\ 0.5]^T$ m without and with appropriate selection of active secondary sources. The active secondary sources are indicated by the filled loudspeaker symbols.

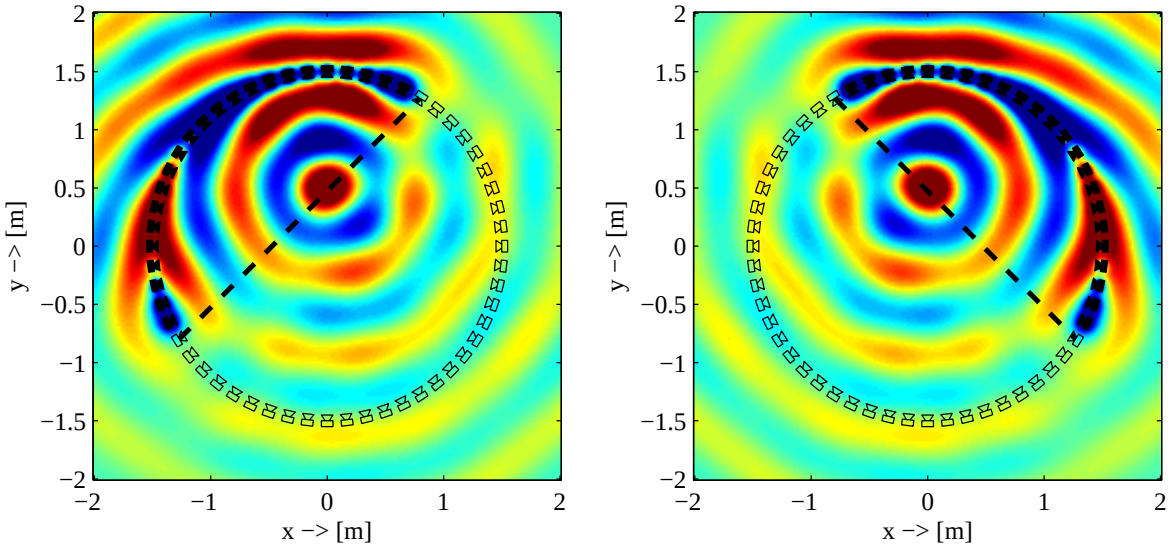

(a) main propagation direction $\alpha_{\text{fs}} = -45^{\text{o}}$

(b) main propagation direction $\alpha_{\text{fs}} = -135^{\text{o}}$

Fig. 10: Wave field reproduced for a monochromatic focused source ($f = 500$ Hz) placed at $\mathbf{x}_{\text{fs}} = [0\ 0.5]^T$ m for two different normal vectors $\mathbf{n}_{\text{fs}} = [\cos(\alpha_{\text{fs}})\ \sin(\alpha_{\text{fs}})]^T$, where α_{fs} denotes the main propagation direction.

countermeasures on a qualitative level. For this purpose the truncation artifacts and proposed countermeasures for linear secondary source contours are briefly reviewed in the following subsection.

5.1. Linear Secondary Source Contours

The effect of truncating the length of a linear secondary source distribution can be qualitatively understood as the effect a gap has on a propagating wave field. Two effects can be observed [14]: (1) the area of the correctly reproduced wave field is limited by the finite aperture and (2) circular waves propagate from the outer secondary sources. The first effect can be described by ray theory, the latter by diffraction theory.

Figure 11(a) shows the wave field reproduced for a point source located at $\mathbf{x}_{\text{ps}} = [0\ \ -1]^T$ m using the linear array from Fig. 7(b) ($\Delta x = 15cm$, $L = 2.10m$). It can be seen that the reproduced wave field contains truncation artifacts. It has been shown that these artifacts can be limited by applying a weight (tapering window) to the secondary source driving signals. Figure 11(b) shows the reproduced wave field when applying a one-sided squared cosine window to the loudspeaker driving signals. The squared cosine part has a width of 25% of the total array length. The truncation artifacts are now reduced, however the effective listening area is also reduced.

A quantitative analysis of the truncation artifacts can be performed by multiplying the driving function for an infinite long distribution with a rectangular window function. The effect of windowing is conveniently analyzed in the spatial frequency domain. A rectangular window function has an infinite bandwidth (sinc-shape) in this domain, leading to high frequency contributions in the spatial frequency domain. Applying a smooth tapering window effectively limits these high frequency components.

Traditionally the tapering of the driving function is independent from the virtual source position. The next section extends this principle to bend and closed-contour secondary source contours.

5.2. Closed Secondary Source Contours

In some situations truncation artifacts will also be present for bend and closed-contour secondary source contours. For a non-closed bend secondary source contour the effects of truncation will be quite similar to the case of linear secondary source contours, if all secondary sources contribute to the reproduction. As outlined in the previous section,

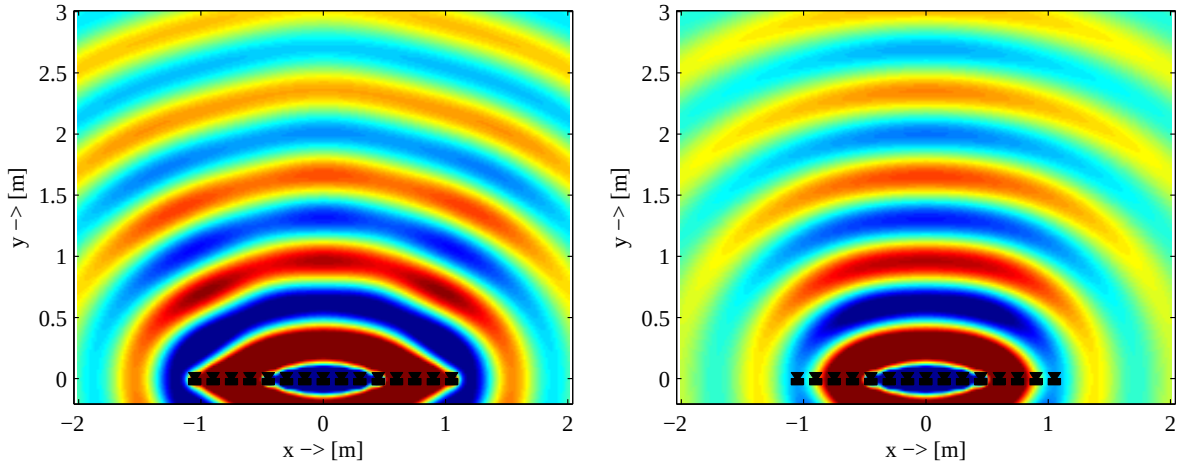

(a) without tapering (b) with tapering

Fig. 11: Wave field reproduced for a monochromatic point source ($f = 500$ Hz) at $\mathbf{x}_{\text{ps}} = [0\ -1]^T$ m without and with tapering of the secondary sources.

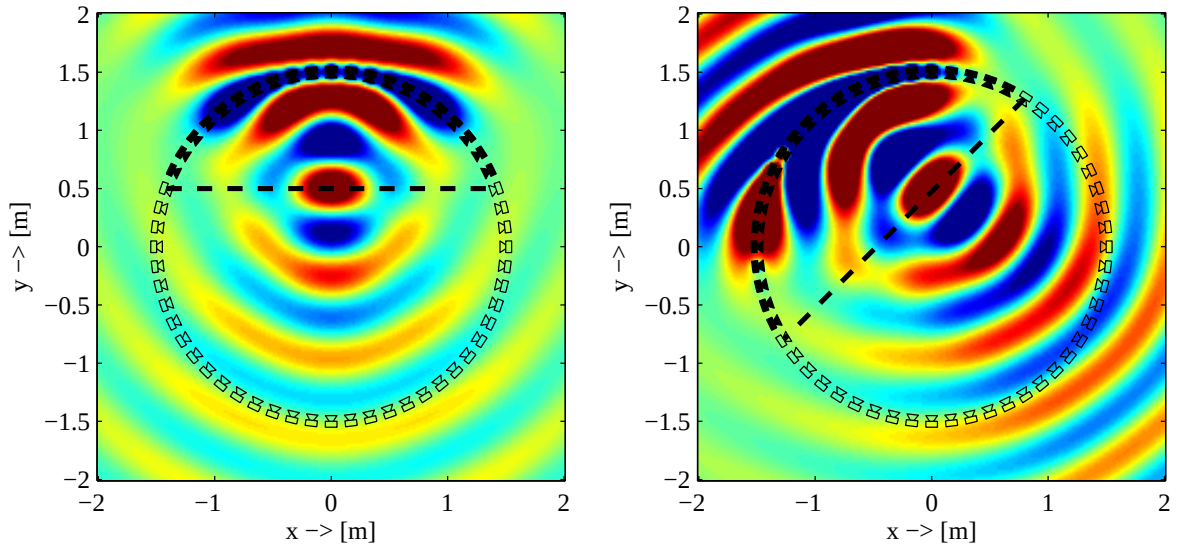

(a) main propagation direction $\alpha_{\text{fs}} = -90^{\text{o}}$ (b) main propagation direction $\alpha_{\text{fs}} = -45^{\text{o}}$

Fig. 13: Wave field reproduced for a monochromatic focused source ($f = 500$ Hz) placed at $\mathbf{x}_{\text{fs}} = [0\ 0.5]^T$ m for two different normal vectors $\mathbf{n}_{\text{fs}}$ with tapering.

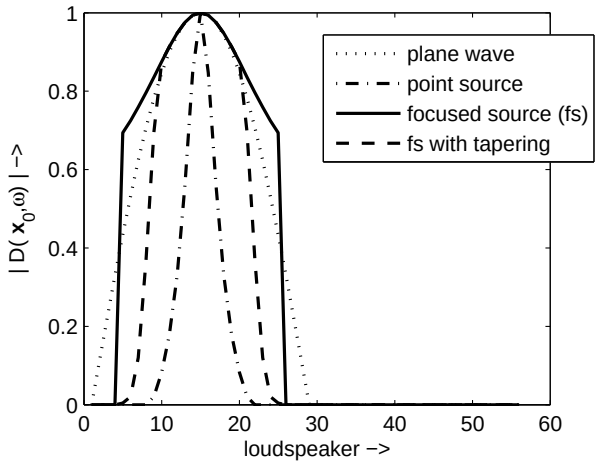

Fig. 12: Absolute value of the driving function $D(\mathbf{x}_0, \omega)$ for the reproduction of a plane wave, a point source and a focused point source on a circular secondary source contour (see Fig. 4(b), 6(b) and 9(b)).

truncation artifacts can be understood as artifacts emerging from truncation of the driving function of an infinitely long array. Hence, truncation artifacts might also be present due to the secondary source selection schemes since these can also be understood as spatial windowing. However, the occurrence of truncation artifacts in this situation depends on the actual driving function. This will be shown qualitatively in the following.

Figure 12 shows the absolute value of the driving function $D(\mathbf{x}_0, \omega)$ for the reproduction of a plane wave, a point source and a focused source on a circular secondary source contour. The shown driving functions have been used for the simulations shown in Fig. 4(b), 6(b) and 9(b), respectively. Both the plane wave and point source driving function have a smooth transition towards the boundaries of the active secondary sources. As a result, almost no truncation artifacts are visible within the listening area in Fig. 4(b) and 6(b). The driving function of the focused source however, exhibits discontinuities at the boundaries of the active secondary sources. As a result, severe truncation artifacts are present in Fig. 9(b). These can be limited by applying a tapering window to the driving function. The tapering window has to be applied only to that part of the driving function where the secondary sources are active. Figure 12 also shows the effect of applying a one-sided squared cosine window to the secondary source driving function of the focused source. The cosine squared part of the window has a width of 25%. It can be seen that the transition towards the ends of the active sources is now smoother. Figure 13(a) shows the reproduced wave field when applying the tapering window. The truncation artifacts are alleviated highly. Figure 13(b) additionally shows the application of the tapering window to the situation illustrated in Fig. 10(a). The tapering effectively limits the truncation artifacts. However, it can also be seen that the listening area is smaller in comparison to applying no tapering.

It can be concluded that truncation artifacts for bend and closed-contour linear secondary source contours call for an tapering window which depends on the active secondary sources and the actual virtual source to be reproduced. A well designed tapering window can efficiently reduce the truncation artifacts.

6. CONCLUSION

This paper presents an analytic secondary source selection criterion for WFS. It has been shown that the proposed criterion is in conjunction with the selection schemes applied in current state of the art implementations for plane waves and point sources. The criterion has been extended towards data-based rendering on basis of the plane wave decomposition and focused sources. The criterion for focused sources opens up a new degree of freedom by incorporating the main propagation direction of the focused source for selection of active secondary sources. All the proposed selection schemes have been implemented into a real-time WFS rendering system (Soundscape Renderer) at the Deutsche Telekom Laboratories. Informal listening tests have proven that the proposed selection criteria create the desired perceptual effect.

Note, that the theory presented so far is not limited to two-dimensional WFS. The mathematical formulations of the secondary source selection criteria in this paper already include the three-dimensional case. Future work includes comparison of the derived criteria with the intrinsic selection of active secondary source performed by approaches like higher-order Ambisonics [15, 16].

7. REFERENCES

[1] Marije A.J. Baalman, "Discretization of complex sound sources for reproduction with wave field synthesis," in *31. Deutsche Jahrestagung für Akustik*, Munic, Germany, 2005.

[2] E. Corteel, "Synthesis of directional sources using wave field synthesis, possibilities, and limitations," *EURASIP Journal on Advances in Signal Processing*, vol. 2007, 2007, Article ID 90509.

[3] S. Spors, "An analytic secondary source selection criteria for wave field synthesis," in *33rd German Annual Conference on Acoustics (DAGA)*, Stuttgart, Germany, March 2007.

[4] E.G. Williams, *Fourier Acoustics: Sound Radiation and Nearfield Acoustical Holography*, Academic Press, 1999.

[5] S. Spors, *Active Listening Room Compensation for Spatial Sound Reproduction Systems*, Ph.D. thesis, University of Erlangen-Nuremberg, 2006.

[6] R. Rabenstein and S. Spors, "Wave field synthesis techniques for spatial sound reproduction," in *Topics in Acoustic Echo and Noise Control*, E.Haensler and G.Schmidt, Eds., chapter 13, pp. 517–545. Springer, 2006.

[7] E. Hulsebos, *Auralization using Wave Field Synthesis*, Ph.D. thesis, Delft University of Technology, 2004.

[8] S. Spors and R. Rabenstein, "Spatial aliasing artifacts produced by linear and circular loudspeaker arrays used for wave field synthesis," in *120th AES Convention*, Paris, France, May 2006, Audio Engineering Society (AES).

[9] E.N.G. Verheijen, *Sound Reproduction by Wave Field Synthesis*, Ph.D. thesis, Delft University of Technology, 1997.

[10] E. Hulsebos, D. de Vries, and E. Bourdillat, "Improved microphone array configurations for auralization of sound fields by Wave Field Synthesis," in *110th AES Convention*, Amsterdam, Netherlands, May 2001, Audio Engineering Society (AES).

[11] S. Yon, M. Tanter, and M. Fink, "Sound focusing in rooms: the time-reversal approach," *Journal of the Acoustical Society of America*, vol. 113, no. 3, pp. 1533–1543, March 2003.

[12] M. Fink, "Time reversal of ultrasonic fields – Part I: Basic principles," *IEEE Transactions on Ultrasocics, Ferroelectrics, and Frequency Control*, vol. 39, no. 5, pp. 555–566, Sept. 1992.

[13] P. Vogel, *Application of Wave Field Synthesis in Room Acoustics*, Ph.D. thesis, Delft University of Technology, 1993.

[14] M.M. Boone, Verheijen E.N.G., and P. van Tol, "Spatial sound-field reproduction by wave-field synthesis," *Journal of the AES*, vol. 43, no. 12, December 1995.

[15] M.A. Poletti, "Three-dimensional surround sound systems based on spherical harmonics," *Journal of the AES*, vol. 53, no. 11, pp. 1004–1025, November 2005.

[16] J. Daniel, R. Nicol, and S. Moreau, "Further investigations of high order ambisonics and wavefield synthesis for holophonic sound imaging," in *114th AES Convention*, Amsterdam, The Netherlands, March 2003, Audio Engineering Society (AES).